doi:10.1093/brain/awr298 Brain 2012: 135; 181–189 | 181

BRAIN
A JOURNAL OF NEUROLOGY

Blood–brain barrier P-glycoprotein function in Alzheimer's disease

Daniëlle M. E. van Assema,[1,2] Mark Lubberink,[1,3] Martin Bauer,[4] Wiesje M. van der Flier,[2] Robert C. Schuit,[1] Albert D. Windhorst,[1] Emile F. I. Comans,[1] Nikie J. Hoetjes,[1] Nelleke Tolboom,[1] Oliver Langer,[4] Markus Müller,[4] Philip Scheltens,[2] Adriaan A. Lammertsma[1] and Bart N. M. van Berckel[1]

1 Department of Nuclear Medicine and PET Research, VU University Medical Center, PO Box 7057, 1007 MB Amsterdam, The Netherlands
2 Department of Neurology and Alzheimer Center, VU University Medical Center, PO Box 7057, 1007 MB Amsterdam, The Netherlands
3 PET Centre, Uppsala University Hospital, 751 85 Uppsala, Sweden
4 Department of Clinical Pharmacology, Medical University of Vienna, Waehringer-Guertel 18-20, A-1090, Vienna, Austria

Correspondence to: D.M.E. van Assema,
Department of Neurology,
Alzheimer Centre,
PK-1Z035,
VU University Medical Centre,
PO Box 7057,
1007 MB Amsterdam, The Netherlands
E-mail: d.vanassema@vumc.nl

A major pathological hallmark of Alzheimer's disease is accumulation of amyloid-β in senile plaques in the brain. Evidence is accumulating that decreased clearance of amyloid-β from the brain may lead to these elevated amyloid-β levels. One of the clearance pathways of amyloid-β is transport across the blood–brain barrier via efflux transporters. P-glycoprotein, an efflux pump highly expressed at the endothelial cells of the blood–brain barrier, has been shown to transport amyloid-β. P-glycoprotein function can be assessed *in vivo* using (*R*)-[^{11}C]verapamil and positron emission tomography. The aim of this study was to assess blood–brain barrier P-glycoprotein function in patients with Alzheimer's disease compared with age-matched healthy controls using (*R*)-[^{11}C]verapamil and positron emission tomography. In 13 patients with Alzheimer's disease (age 65 ± 7 years, Mini-Mental State Examination 23 ± 3), global (*R*)-[^{11}C]verapamil binding potential values were increased significantly ($P = 0.001$) compared with 14 healthy controls (aged 62 ± 4 years, Mini-Mental State Examination 30 ± 1). Global (*R*)-[^{11}C]verapamil binding potential values were 2.18 ± 0.25 for patients with Alzheimer's disease and 1.77 ± 0.41 for healthy controls. In patients with Alzheimer's disease, higher (*R*)-[^{11}C]verapamil binding potential values were found for frontal, parietal, temporal and occipital cortices, and posterior and anterior cingulate. No significant differences between groups were found for medial temporal lobe and cerebellum. These data show altered kinetics of (*R*)-[^{11}C]verapamil in Alzheimer's disease, similar to alterations seen in studies where P-glycoprotein is blocked by a pharmacological agent. As such, these data indicate that P-glycoprotein function is decreased in patients with Alzheimer's disease. This is the first direct evidence that the P-glycoprotein transporter at the blood–brain barrier is compromised in sporadic Alzheimer's disease and suggests that decreased P-glycoprotein function may be involved in the pathogenesis of Alzheimer's disease.

Keywords: P-glycoprotein; blood–brain barrier; PET; Alzheimer's disease; (*R*)-[^{11}C]verapamil

Abbreviations: BP_{ND} = binding potential$_{non\text{-}displaceable}$; PIB = Pittsburgh compound B

Received April 5, 2011. Revised August 10, 2011. Accepted September 3, 2011. Advance Access publication November 26, 2011

Introduction

Alzheimer's disease is the most common form of dementia (Cummings, 2004). A major pathological hallmark of Alzheimer's disease is the deposition of amyloid-β plaques in the brain (Braak and Braak, 1991). Amyloid-β pathology can be visualized and quantified *in vivo* using [^{11}C]Pittsburgh compound B (PIB) and PET (Klunk *et al*., 2004; Tolboom *et al*., 2009*b*).

The origin of amyloid-β depositions in Alzheimer's disease is unclear. The amyloid hypothesis proposes that it may be caused by an imbalance between amyloid-β production and clearance (Hardy and Selkoe, 2002). In familial Alzheimer's disease, which accounts for <5% of all cases, there is evidence of life-long increased production of amyloid-β due to genetic alterations (Blennow *et al*., 2006). In the far more common sporadic Alzheimer's disease, however, a failure to clear amyloid-β from the brain is thought to play an important role in the pathogenesis of the disease (Mawuenyega *et al*., 2010). Mechanisms involved in clearing amyloid-β from the brain include degradation by a variety of proteases, removal through the interstitial fluid-CSF bulk flow into the bloodstream, perivascular lymphatic drainage and transport across the blood–brain barrier (Weller *et al*., 2008). Although the exact cause of reduced clearance of amyloid-β from the brain in sporadic Alzheimer's disease remains unclear, several leads point towards a regulatory role for the blood–brain barrier (Zlokovic *et al*., 2000; Deane and Zlokovic, 2007).

The blood–brain barrier, composed of a monolayer of brain capillary endothelial cells, serves to maintain in the CNS and protects the brain from toxic substances. These blood–brain barrier functions are realized through different mechanisms, such as tight junctions between adjacent endothelial cells to prevent entry of compounds into the brain, and active efflux mechanisms to transport endogenous and exogenous substances from the brain to the blood (Loscher and Potschka, 2005). Due to the presence of tight junctions between cerebrovascular endothelial cells, the transport of amyloid-β across the blood–brain barrier requires carrier- or receptor-mediated transport systems. The receptor for advanced glycation end products is a primary transporter of amyloid-β from the systemic circulation across the blood–brain barrier into the brain, whereas the low-density lipoprotein receptor-related protein-1 (LRP1) is one of the transporters involved in the transport of amyloid-β out of the brain (Deane *et al*., 2004, 2009; Donahue *et al*., 2006).

Recently, it has been suggested that P-glycoprotein, a 170 kDa plasma membrane protein encoded in humans by the multi-drug resistance 1 gene (MDR1 or ABCB1) and belonging to the family of ATP-binding cassette transporters, is also involved in the clearance of amyloid-β from brain. P-glycoprotein is expressed in organs with an excretory and/or barrier function, such as intestine, liver, kidney and the blood–brain barrier. At the blood–brain barrier, P-glycoprotein is highly expressed at the luminal side of the endothelial cells (Demeule *et al*., 2001), where it acts as an efflux transporter, extruding substances from the brain to the blood (de Lange, 2004; Lee and Bendayan, 2004). Being able to transport a broad spectrum of substrates, P-glycoprotein has been shown to play an important role in maintaining homoeostasis in the CNS, thereby protecting the brain from accumulation of potentially toxic substances (Schinkel, 1999; Fromm, 2004).

The evidence that amyloid-β is also a substrate for P-glycoprotein is based on several studies. For instance, it has been shown *in vitro* that P-glycoprotein transports amyloid-β and that blocking P-glycoprotein function decreases transport of amyloid-β (Lam *et al*., 2001; Kuhnke *et al*., 2007). Furthermore, amyloid-β depositions are inversely correlated with P-glycoprotein expression in the brain of elderly non-demented humans (Vogelgesang *et al*., 2002). In addition, in an Alzheimer's disease mouse model, knocking out blood–brain barrier P-glycoprotein expression increased amyloid-β depositions (Cirrito *et al*., 2005), while restoring blood–brain barrier P-glycoprotein expression and transport activity reduced brain amyloid-β levels (Hartz *et al*., 2010). At present, there is no *in vivo* information on P-glycoprotein function in sporadic Alzheimer's disease.

P-glycoprotein function can be assessed *in vivo* using the PET tracer [^{11}C]verapamil (Hendrikse *et al*., 1999, 2001; Bart *et al*., 2003). [^{11}C]verapamil enters the brain through passive diffusion and, at the low concentrations used in PET, is a substrate for P-glycoprotein (Ambudkar *et al*., 1999; Tournier *et al*., 2011). The validity of [^{11}C]verapamil as a PET tracer for assessing P-glycoprotein function was further demonstrated by increased cerebral retention of [^{11}C]verapamil following blockade of P-glycoprotein with cyclosporine (Sasongko *et al*., 2005; Lee *et al*., 2006). [^{11}C]verapamil has often been used in its racemic form, as both (*R*) and (*S*) enantiomers are substrates for P-glycoprotein. Nevertheless, for quantification of P-glycoprotein function, a pure enantiomer is required. As (*R*)-[^{11}C]verapamil is metabolized less in the human body than (*S*)-[^{11}C]verapamil, it is considered to be the preferred isomer (Luurtsema *et al*., 2003) and the brain retention of (*R*)-[^{11}C]verapamil is thought to be inversely related to blood–brain barrier P-glycoprotein function. Using [^{11}C]verapamil and PET, it has been shown that blood–brain barrier P-glycoprotein function decreases in normal ageing and in neurodegenerative diseases such as progressive supranuclear palsy and multiple system atrophy, with conflicting results in Parkinson's disease (Toornvliet *et al*., 2006; Bartels *et al*., 2008*a*, *b*, 2009; Bauer *et al*., 2009). As decreased clearance of amyloid-β from the brain is thought to be a major cause of amyloid-β accumulation in the pathogenesis of sporadic Alzheimer's disease, together with the fact that P-glycoprotein is able to transport amyloid-β, the purpose of this study was to measure blood–brain barrier P-glycoprotein function *in vivo* using (*R*)-[^{11}C]verapamil PET in patients with sporadic Alzheimer's disease and healthy controls. The hypothesis was that P-glycoprotein function is reduced in patients with Alzheimer's disease, so that an increase in binding potential$_{\text{non-displaceable}}$ (BP_{ND}) of (*R*)-[^{11}C]verapamil is expected in patients with Alzheimer's disease compared with healthy controls.

Materials and methods

Participants

Fifteen subjects with probable Alzheimer's disease and 14 age-matched healthy controls were included in this study. Patients with

Alzheimer's disease with mild to moderate disease (Mini-Mental State Examination scores ⩾20; Folstein *et al*., 1975) were recruited from the out-patient Memory Clinic of the Alzheimer Centre of the VU University Medical Centre, Amsterdam. All subjects received a standard dementia screening that included medical history, physical and neurological examinations, screening laboratory tests, and brain MRI. Clinical diagnosis of probable Alzheimer's disease was established by consensus in a multidisciplinary meeting according to the criteria proposed by the National Institute of Neurological and Communicative Disorders and Stroke and the Alzheimer's Disease and Related Disorders Association (NINCDS-ADRDA) (McKhann *et al*., 1984). To confirm the presence of Alzheimer's disease pathology in the brain, increased cortical accumulation of [^{11}C]PIB PET was required for patients with Alzheimer's disease (Tolboom *et al*., 2010). Controls were recruited by means of flyers and through advertisements in newspapers. Controls had normal cognitive function with normal Mini-Mental State Examination scores (>26). Exclusion criteria for all participants were history of any major psychiatric or neurological illness (other than Alzheimer's disease). None of the healthy controls used medication. Five of the patients with Alzheimer's disease were being treated with acetylcholinesterase inhibitors. Acetylcholinesterase inhibitors are not known to be transported by P-glycoprotein or interfere with P-glycoprotein function (Bart *et al*., 2000; Didziapetris *et al*., 2003). Two patients with Alzheimer's disease were on low doses of antidepressant medication, which possibly are substrates for P-glycoprotein (Uhr *et al*., 2000; Uhr and Grauer, 2003), one patient using citalopram 20 mg/day, the other nortriptyline 10 mg/day. Additional exclusion criteria for controls were subjective memory complaints or clinically significant abnormalities on brain MRI as determined by a neuroradiologist. The study was approved by the Medical Ethics Review Committee of the VU University Medical Centre. Written informed consent was obtained from all subjects after a complete written and verbal description of the study.

Magnetic resonance imaging

All subjects underwent structural MRI using a 1.5 T Sonata scanner (Siemens Medical Solutions), except four of the healthy male subjects, who were scanned using a 1.0 T Magnetom Impact scanner (Siemens Medical Solutions). The scan protocol on both MRI scanners was identical and included a coronal T_1-weighted 3D MPRAGE (magnetization prepared rapid acquisition gradient echo; slice thickness 1.5 mm, 160 slices, matrix size 256 × 256; voxel size of 1 × 1 × 1.5 mm; echo time = 3.97 ms; repetition time = 2.700 ms; inversion time = 950 ms; flip angle 8°), which was used for co-registration and region of interest definition.

Positron emission tomography data acquisition

PET scans were performed on an ECAT EXACT HR+ scanner (Siemens/CTI), equipped with a neuro-insert to reduce the contribution from outside field of view activity. This scanner enables the acquisition of 63 transaxial planes over a 15.5 cm axial field of view, allowing the whole brain to be imaged in a single bed position. The properties of this scanner have been reported elsewhere (Brix *et al*., 1997). All subjects received an indwelling radial artery cannula for arterial blood sampling and a venous cannula for tracer injection. Prior to tracer injection, a 10 min transmission scan in 2D acquisition mode was performed using three retractable rotating ^{68}Ge rod sources. This scan was used to correct the subsequent emission scan for photon attenuation. Next, a dynamic emission scan in 3D acquisition mode was started simultaneously with a bolus injection of (*R*)-[^{11}C]verapamil. The synthesis of (*R*)-[^{11}C]verapamil has been described previously (Luurtsema *et al*., 2002). Using an infusion pump (Med-Rad), radiotracer injection was performed at a rate of 0.8 ml/s, followed by a flush of 42 ml saline at 2.0 ml/s. The dynamic emission scan consisted of 20 frames with progressive increase in frame duration (1 × 15, 3 × 5, 3 × 10, 2 × 30, 3 × 60, 2 × 150, 2 × 300, 4 × 600 s) and a total duration of 60 min. Patient movement was restricted by the use of a head holder and monitored by checking the position of the head using laser beams. Using an on-line blood sampler (Veenstra Instruments), arterial blood was withdrawn continuously at a rate of 5 ml/min during the first 5 min and 2.5 ml/min during the rest of the scan. At 2.5, 5, 10, 20, 30, 40 and 60 min after tracer injection, continuous blood sampling was interrupted briefly to collect additional manual blood samples. After each sample, the arterial line was flushed with a heparinized saline solution. These manual samples were used to determine plasma to whole blood radioactivity concentration ratios. In addition, fractions of parent (*R*)-[^{11}C]verapamil and its radioactive polar metabolites in plasma were determined using a combination of solid-phase extraction and high-pressure liquid chromatography, as described previously (Luurtsema *et al*., 2005).

On the same day, patients with Alzheimer's disease underwent a second PET scan following injection of [^{11}C]PIB in order to confirm amyloid-β pathology in the brain. This dynamic 90 min scan was acquired as described previously (Tolboom *et al*., 2009*a*).

Positron emission tomography data analysis

All PET data were corrected for attenuation, randoms, dead time, scatter and decay. Images were reconstructed using a standard filtered back projection algorithm applying a Hanning filter with a cut-off at 0.5 times the Nyquist frequency. A zoom factor of 2 and a matrix size of 256 × 256 × 63 were used, resulting in a voxel size of 1.2 × 1.2 × 2.4 mm and a spatial resolution of ∼6.5 mm full width at half maximum at the centre of the field of view. Co-registration of structural T_1-magnetic resonance images to corresponding PET images (using summed images of frames 3–12) and segmentation of the co-registered MRI into grey matter, white matter and CSF was performed using statistical parametrical mapping (SPM, version SPM2, www.fil.ion.ucl.ac.uk/spm, Institute of Neurology). Regions of interest were defined based on the segmented MRI using a probabilistic template as implemented in PVElab (Svarer *et al*., 2005). PET data were not corrected for partial volume effects. Regions of interest were mapped onto the dynamic PET images and regional time-activity curves were generated. For (*R*)-[^{11}C]verapamil scans, the original on-line blood curve was calibrated using whole blood radioactivity concentrations of the seven manual samples. The calibrated whole blood curve was multiplied with a single-exponential fit to the plasma to whole blood ratio, thereby generating a total plasma curve. Finally, the metabolite corrected plasma input function was obtained by multiplying the total plasma curve with one minus the polar metabolite fraction fitted to a sigmoid function (Gunn *et al*., 1998).

Kinetic analyses were performed using software developed within Matlab 7.04 (The Mathworks). First, (*R*)-[^{11}C]verapamil data were analysed using spectral analysis, a technique that produces a spectrum of the kinetic components that are needed to relate tissue response to plasma input function without making *a priori* assumptions regarding

the number of compartments (Cunningham and Jones, 1993). This method is based on the assumption that the tissue response to a unit impulse (impulse response function; IRF) can be described as a linear combination of a limited number of predefined exponentially decaying basis functions:

$$\mathrm{IRF}(t) = \sum_i \alpha_i \exp(-\beta_i t) \quad (1)$$

In the present analysis, 50 basis functions with logarithmically spaced β_i ranging from 0.015 to 2 min^{-1} were used. The measured tissue curve $C_T(t)$ is then described as the convolution of IRF(t) with the plasma input function $C_P(t)$ plus a blood volume term:

$$C_T(t) = \sum_i C_P(t) \otimes \alpha_i \exp(-\beta_i t) + V_B(t) C_B(t) \quad (2)$$

Equation 2 can be solved by non-negative least-squares, yielding a limited number of $\alpha_i > 0$, representing the number of tissue compartments necessary to describe the data. For any number of compartments, the parameters α and β can be expressed in terms of rate constants of a conventional compartment model with a similar number of compartments, and vice versa.

Based on the results of spectral analysis, (*R*)-[^{11}C]verapamil data were also analysed using non-linear regression of the standard two tissue compartment model including a blood volume component, yielding, in addition to the individual rate constants ($K_1 - k_4$) between compartments, the outcome measure BP_{ND} (Innis *et al*., 2007). BP_{ND} (= k_3/k_4) is the non-displaceable binding potential of verapamil. Starting values for the parameters in the non-linear regression analysis were based on the results of spectral analysis. To obtain robust BP_{ND} values, the non-specific distribution volume K_1/k_2 was first determined for a whole brain grey matter region of interest and then assumed to be the same for all grey matter regions of interest (Kropholler *et al*., 2005). BP_{ND} of frontal (volume-weighted average of orbital frontal, medial inferior frontal and superior frontal), parietal, temporal (volume-weighted average of superior temporal and medial inferior temporal), occipital, medial temporal lobe (volume-weighted average of entorhinal cortex and hippocampus) and cerebellar cortices and posterior and anterior cingulate was used. In addition, a global cortical region was defined consisting of the volume-weighted average of frontal, parietal, temporal and occipital cortices and anterior and posterior cingulate.

[^{11}C]PIB PET data were analysed as described previously using 90-min dynamic scans (Tolboom *et al*., 2009*b*). For confirming the presence of amyloid pathology in the brain, [^{11}C]PIB PET scans were assessed visually by an experienced nuclear medicine physician (B.vB.) and classified as either being PIB-positive or -negative (Tolboom *et al*., 2010).

In addition to this visual classification, [^{11}C]PIB data were quantified for the same regions of interest as used for the quantitative analysis of (*R*)-[^{11}C]verapamil data. BP_{ND} of [^{11}C]PIB was derived for these regions of interest using the simplified reference tissue model (SRTM; Lammertsma and Hume, 1996; Tolboom *et al*., 2009*a*) with cerebellar grey matter as reference tissue.

Statistical analysis

Data are presented as mean ± standard deviation (SD), unless otherwise stated. Group differences were calculated using non-parametric Mann–Whitney U-tests. A $P < 0.05$ was considered significant. The relationship between BP_{ND} of (*R*)-[^{11}C]verapamil and BP_{ND} of [^{11}C]PIB was assessed using Spearman's correlation coefficient.

Results

(*R*)-[^{11}C]verapamil PET studies were performed in 15 patients with Alzheimer's disease and 14 healthy controls. [^{11}C]PIB scans were acquired for all patients with Alzheimer's disease and three healthy controls. Of the 15 patients with Alzheimer's disease, 13 were classified as being PIB positive and two as PIB negative. The two PIB-negative patients were excluded from the Alzheimer's disease group for further analysis. Controls who underwent a [^{11}C]PIB scan were PIB negative.

There were no differences between groups with respect to age, sex, injected dose and specific activity of (*R*)-[^{11}C]verapamil (Table 1). As expected, patients with Alzheimer's disease had significantly lower Mini-Mental State Examination scores than healthy controls.

Spectral analysis of (*R*)-[^{11}C]verapamil data clearly showed the presence of two components in both patients with Alzheimer's disease and healthy controls. In healthy controls, these two components had clearance rates of $0.039 \pm 0.010\ \mathrm{min}^{-1}$ and $0.43 \pm 0.42\ \mathrm{min}^{-1}$ for global cortical region. In patients with Alzheimer's disease for global cortical region, clearance rates of $0.040 \pm 0.008\ \mathrm{min}^{-1}$ and $0.77 \pm 0.49\ \mathrm{min}^{-1}$ were found. For the latter component, a significantly faster clearance rate was found in Alzheimer's disease (Fig. 1, $P = 0.0003$). Because of these spectral analysis findings, a two tissue compartment model was implemented and used for further quantitative data analysis.

For the global cortical region (Table 2), no significant differences in rate constants K_1, k_2, k_3, and k_4 were found between groups. In addition, rate constants were assessed between groups for frontal, parietal, temporal, occipital, posterior and anterior cingulate, medial temporal lobe and cerebellar regions of interest. For K_1, k_2 and k_4, no significant differences were found between groups. For k_3, significant differences were found in posterior cingulate ($P = 0.020$) and medial temporal lobe ($P = 0.037$) region of interest, with higher values in Alzheimer's disease compared with healthy controls.

Global cortical BP_{ND} of (*R*)-[^{11}C]verapamil was higher in patients with Alzheimer's disease compared with age-matched healthy controls (patients with Alzheimer's disease: 2.18 ± 0.25; healthy controls: 1.77 ± 0.41, $P = 0.001$; Fig. 2). In fact, for the parietal, temporal, occipital and posterior cingulate region of interest,

Table 1 Characteristics of subject groups

Characteristics of subjects groups'	Controls	Alzheimer's disease	*P*-value
n	14	13	
Age (years)	62 ± 4	65 ± 7	0.29
Male/female (% female)	8/6 (43)	10/3 (23)	0.29
MMSE	30 ± 1	23 ± 3	<0.000
Injected dose (MBq)	378 ± 31	354 ± 36	0.10
Specific activity (GBq/μmol)	40 ± 13	46 ± 29	0.98

Differences between groups were calculated using Mann–Whitney U-tests. MMSE = Mini-Mental State Examination; Injected dose = injected dose of (*R*)-[^{11}C]verapamil; Specific activity = specific activity of (*R*)-[^{11}C]verapamil.

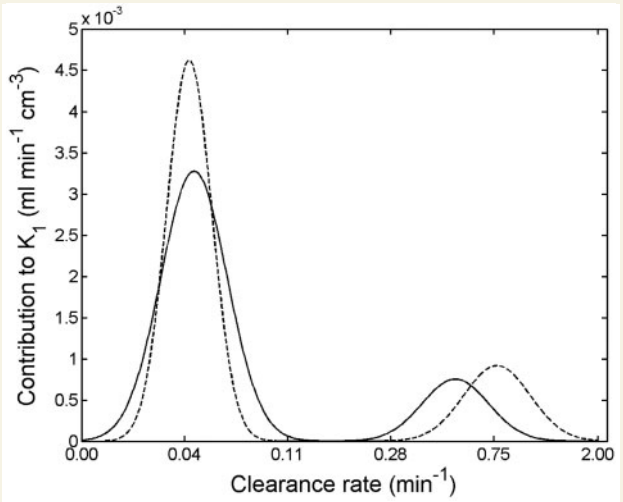

Figure 1 Results of spectral analysis. Clearance rates on the *x*-axis correspond to the clearance rates β_i of the basis functions in Equations (1) and (2), and contribution to K_1 on the *y*-axis corresponds to the parameters α_i. Lines represent fits of two Gaussian functions through the mean spectrum of all regions of interest from 14 healthy controls (solid line) and 13 patients with Alzheimer's disease (dashed line).

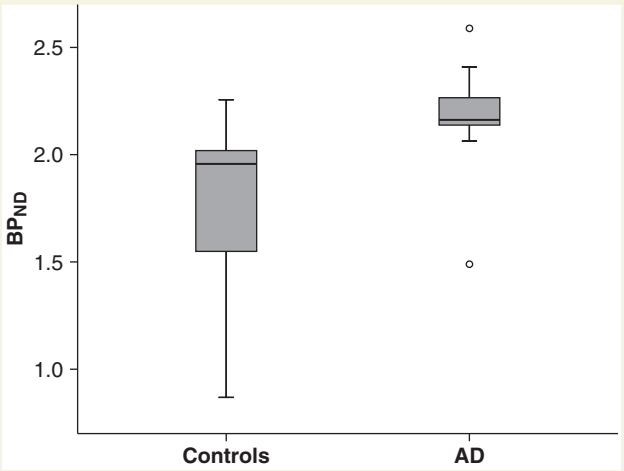

Figure 2 Boxplot for (*R*)-[^{11}C]verapamil BP_{ND} of the global cortical region. The Alzheimer's disease group (*right*) shows increased BP_{ND} compared with the healthy control group (*left*) ($P = 0.001$). BP_{ND} = binding potential of (*R*)-[^{11}C]verapamil; open circles = outliers.

Table 2 Individual (*R*)-[^{11}C]verapamil rate constants for the global cortical region

Constant	Controls	Alzheimer's disease	*P*-value
K_1	0.05 ± 0.01	0.05 ± 0.01	0.40
k_2	0.14 ± 0.05	0.17 ± 0.03	0.56
k_3	0.16 ± 0.10	0.26 ± 0.08	0.16
k_4	0.09 ± 0.04	0.12 ± 0.03	0.65

Group differences were calculated using Mann–Whitney U-tests.

Table 3 BP_{ND} of (*R*)-[^{11}C]verapamil for several cortical brain regions

Brain region	Controls	Alzheimer's disease	*P*-value
Global	1.77 ± 0.41	2.18 ± 0.25	0.001
Frontal	1.79 ± 0.40	2.12 ± 0.28	0.029
Parietal	1.70 ± 0.37	2.15 ± 0.26	0.000
Temporal	1.84 ± 0.46	2.29 ± 0.27	0.000
Occipital	1.75 ± 0.38	2.20 ± 0.25	0.001
Posterior cingulate	1.65 ± 0.30	2.20 ± 0.35	0.000
Anterior cingulate	1.67 ± 0.50	2.06 ± 0.35	0.029
Medial temporal lobe	2.51 ± 0.79	2.97 ± 0.42	0.120
Cerebellum	1.87 ± 0.57	1.99 ± 0.24	0.109

Group differences were calculated using Mann–Whitney U-tests.

significantly higher BP_{ND} values were found in Alzheimer's disease compared with healthy controls. Also for frontal and anterior cingulate regions of interest, significantly higher BP_{ND} values were found in Alzheimer's disease, though the differences for these regions were smaller (Table 3). There were no between-group differences for medial temporal lobe and cerebellum. In the two PIB-negative patients, (*R*)-[^{11}C]verapamil BP_{ND} values were in the range of the PIB-positive patients with Alzheimer's disease with global BP_{ND} values for (*R*)-[^{11}C]verapamil of 2.18 and 2.15, respectively.

No significant associations were found between BP_{ND} of (*R*)-[^{11}C]verapamil and BP_{ND} of [^{11}C]PIB.

Discussion

The main finding of this study is an increased (*R*)-[^{11}C]verapamil BP_{ND} in the brain of patients with Alzheimer's disease as compared with values in healthy age-matched controls. For the global cortical region, this increase was ~23% and in some smaller regions like posterior cingulate, there was an even larger increase of 33%. This suggests reduced P-glycoprotein function at the blood–brain barrier in patients with Alzheimer's disease, not only at a regional, but also at a global level. To the best of our knowledge, this is the first *in vivo* evidence that blood–brain barrier P-glycoprotein transporter dysfunction occurs in sporadic Alzheimer's disease.

In both patients with Alzheimer's disease and healthy controls, spectral analysis, a data driven technique, indicated that (*R*)-[^{11}C]verapamil data were best described using a two compartment model. This is in contrast to a previous study in healthy volunteers, in which a one compartment model was generally preferred, partly because of its superior test–retest variability (Lubberink *et al*., 2007). In healthy subjects, the need for a second compartment to describe kinetics of (*R*)-[^{11}C]verapamil is especially evident after blocking P-glycoprotein, for example, using cyclosporine-A or tariquidar (Muzi *et al*., 2009; Wagner *et al*., 2009). In the present

study, two compartments for (*R*)-[^{11}C]verapamil were identified, a 'slow' compartment and a 'fast' compartment. The fast compartment contributes only a few per cent to the total volume of distribution of the tracer. In physiological terms, the second compartment is not fully understood. The most logical explanation is that the first compartment represents radiotracer in the vessel wall before it is pumped back into the circulation, while the second represents radiotracer retention in the brain parenchyma. If this is the case, BP_{ND} reflects P-glycoprotein function. This is in line with results of previous studies, where P-glycoprotein inhibition with the very potent P-glycoprotein inhibitor cyclosporine-A or with tariquidar clearly showed an increase in k_3 and, to a lesser extent, in k_4, resulting in an overall increase in BP_{ND} (Muzi *et al*., 2009; Wagner *et al*., 2009).

As the direction of change in BP_{ND} in the patients with Alzheimer's disease in this study is similar to that induced by P-glycoprotein blocking in healthy subjects, the corresponding increase in BP_{ND} can be interpreted as a measure of decreased P-glycoprotein function.

The pathophysiology underlying decreased P-glycoprotein function at the blood–brain barrier in Alzheimer's disease is not known and it is unknown whether P-glycoprotein function decreases prior to the occurrence of amyloid depositions, or whether amyloid plaques have a destructive effect on the blood vessel wall resulting in secondary P-glycoprotein dysfunction. In a post-mortem study (Vogelgesang *et al*., 2004), it was shown that vascular amyloid-β depositions were never co-localized with expression of P-glycoprotein and that in brains with early deposition of amyloid-β in arterioles, capillary P-glycoprotein expression was significantly increased. This suggests that the typically low expression of P-glycoprotein in arteries and arterioles contributes to local amyloid-β deposition, which in turn results in compensatory increases in P-glycoprotein expression in capillaries in an attempt to limit further accumulation. When amyloid-β accumulation increases and capillaries themselves become amyloidotic and lose their P-glycoprotein, this could lead to further accumulation of amyloid-β in the brain. Longitudinal *in vivo* imaging studies of both amyloid deposition and P-glycoprotein function, preferably in combination with other imaging techniques to measure the degree of small vessel disease, could shed some light on this interesting question.

Previously, it has been reported that P-glycoprotein function may play an important role in the clearance of amyloid-β across the blood–brain barrier (Lam *et al*., 2001; Vogelgesang *et al*., 2002; Cirrito *et al*., 2005; Kuhnke *et al*., 2007; Hartz *et al*., 2010). As such, decreased blood–brain barrier P-glycoprotein function may be a crucial factor in the pathogenesis of Alzheimer's disease. This is the first study reporting increased (*R*)-[^{11}C]verapamil BP_{ND} in grey matter in Alzheimer's disease. This may relate to previous studies with (*R*)-[^{11}C]verapamil in healthy ageing, which reported an age-related increase in (*R*)-[^{11}C]verapamil retention in white matter regions of the brain (Bartels *et al*., 2009; Bauer *et al*., 2009). (*R*)-[^{11}C]verapamil BP_{ND} in white matter was not investigated in the present study, as the tracer kinetic models used have not been validated for this purpose. Future studies with validated tracers kinetic models for assessment of white matter P-glycoprotein function should be performed to address the question whether white matter P-glycoprotein function is changed in Alzheimer's disease and to assess it's relation to grey matter P-glycoprotein function. Furthermore, decreased P-glycoprotein function may be involved in other diseases where amyloid deposits are found, such as cerebral amyloid angiopathy, in which amyloid accumulates in blood vessel walls in the brain (Vogelgesang *et al*., 2004; Smith and Greenberg, 2009). Evidence is emerging that Alzheimer's disease pathology frequently co-exists and may be associated with cerebrovascular pathology such as cerebral amyloid angiopathy and arteriosclerotic plaques (Smith and Greenberg, 2009). Using [^{11}C]PIB PET, it has been shown that the occipital-to-global [^{11}C]PIB ratio is significantly increased in patients with cerebral amyloid angiopathy, indicating more pronounced amyloid pathology in occipital lobe in patients with cerebral amyloid angiopathy (Johnson *et al*., 2007). In the present study, increased BP_{ND} of both [^{11}C]PIB and (*R*)-[^{11}C]verapamil was found in most large cortical brain regions in patients with Alzheimer's disease, including the occipital lobe, which supports a possible overlap of Alzheimer's disease pathology with cerebral amyloid angiopathy pathology.

Probing P-glycoprotein function at the blood–brain barrier in the very early stages of amyloid depositions is of crucial importance. If decreased P-glycoprotein function is involved in the pathogenesis of amyloid deposition in Alzheimer's disease, this would implicate that P-glycoprotein may be a potential treatment target and a possible target to modulate disease progression. In a broader sense, P-glycoprotein dysfunction in Alzheimer's disease may be a (surrogate) marker for more widespread blood–brain barrier dysfunction in Alzheimer's disease, involving also other amyloid-β transporters, such as LRP1.

P-glycoprotein is one of the major efflux pumps at the blood–brain barrier involved in transport out of the brain of various drugs and other toxic compounds (Didziapetris *et al*., 2003; de Lange, 2004; Lee and Bendayan, 2004). Consequently, P-glycoprotein dysfunction could make patients with Alzheimer's disease more vulnerable to drug toxicity and CNS side-effects of drugs that enter the brain. Furthermore, decreased P-glycoprotein function could also lead to accumulation of toxic compounds other than amyloid-β by which the brain can be damaged even further. Examples of such compounds are environmental toxins like pesticides. Indeed, it has been shown that efflux of the pesticide endosulfan is mediated by P-glycoprotein (Bain and LeBlanc, 1996). This could be an important mechanism underlying neurodegeneration associated with Alzheimer's disease and other neurodegenerative diseases.

The diagnosis of probable Alzheimer's disease according to NINCDS-ADRDA criteria is a clinical diagnosis with known sensitivity and specificity of about 65 and 75%, respectively (Cummings, 2004). Therefore in this study, [^{11}C]PIB PET scans were performed to support the clinical diagnosis, in this case leading to the exclusion of two patients from our Alzheimer's disease sample. (*R*)-[^{11}C]verapamil BP_{ND} values in the two patients that were visually classified as PIB negative were in the range of the PIB-positive patients with Alzheimer's disease. Quantitatively, however, these two patients did show some amount of increased [^{11}C]PIB binding with RPM2-derived (Yaqub *et al*., 2008) global

[^{11}C]PIB BP_{ND} values of 0.19 and 0.34, respectively. Although this is increased compared with healthy controls, it is still below the threshold of [^{11}C]PIB BP_{ND} of 0.54 for being [^{11}C]PIB positive (Tolboom *et al*., 2010). Interestingly, apart from atrophy coherent with Alzheimer's disease, both patients had significant signs of microvascular pathology on MRI, which by itself is associated with increased [^{11}C]PIB retention (Lee *et al*., 2011): one patient had hallmarks of cerebral amyloid angiopathy, while the other had white matter hyperintensities with beginning confluence of lesions (Fazekas score 2; Fazekas *et al*., 1987). As such, it is conceivable that these patients suffer from mixed pathology in the brain and that microvascular pathology may have contributed to the decreased P-glycoprotein function found in these patients, or vice versa.

No significant correlations were found between BP_{ND} of (*R*)-[^{11}C]verapamil and BP_{ND} of [^{11}C]PIB. This may be due to a ceiling effect of [^{11}C]PIB, as [^{11}C]PIB uptake appears to behave as an on/off phenomenon in patients with Alzheimer's disease, [^{11}C]PIB retention does not reflect disease severity (Engler *et al*., 2006) and [^{11}C]PIB binding does not increase substantially over time (Ossenkoppele *et al*., 2010). Furthermore, (*R*)-[^{11}C]verapamil and [^{11}C]PIB binding showed substantial spatial overlap, although some inconsistencies were also observed. For instance, relatively high [^{11}C]PIB binding was observed in the anterior cingulate and frontal cortex regions of interest, while (*R*)-[^{11}C]verapamil binding was only moderately increased in these regions. As such, there appears to be a regional distribution in the severity of P-glycoprotein dysfunction in Alzheimer's disease. Studies in larger samples are necessary to further address these regional differences and its relation to amyloid depositions. To assess whether there is direct relationship between (*R*)-[^{11}C]verapamil and [^{11}C]PIB accumulation in future studies, subjects would have to be included at the very early stages of amyloid deposition.

The present results cannot be explained by medication-induced P-glycoprotein blockade, as the present cohort of patients with Alzheimer's disease did not use medication that is known to interfere with P-glycoprotein function, and there was no use of medication in the control group. Two patients with Alzheimer's disease used low doses of antidepressant medication, which are P-glycoprotein substrates in mice (Uhr *et al*., 2000; Uhr and Grauer, 2003). Theoretically, these compounds could compete with (*R*)-[^{11}C]verapamil for transport by P-glycoprotein, but exclusion of these patients did not change results (data not shown).

A limitation of this study is the relatively small number of patients with Alzheimer's disease and controls. There is a need to replicate these findings in larger groups of controls and patients at different stages of the disease. Furthermore, amyloid imaging was performed in only 3 of the 14 healthy controls, which showed no increased [^{11}C]PIB uptake. In post-mortem studies, Alzheimer's disease pathology can be found in ~30% of the cognitively healthy elderly subjects and imaging studies also have reported increased [^{11}C]PIB uptake in ~30% of cognitively healthy elderly subjects (Pike *et al*., 2007; Aizenstein *et al*., 2008). Therefore, amyloid deposition in some of the remaining 11 controls cannot be excluded. This will, however, not affect the main finding of reduced P-glycoprotein function in patients with Alzheimer's disease, as inclusion of such healthy controls would tend to reduce the difference between patients with Alzheimer's disease and controls. In the present study, no correction for partial volume effects was applied to the PET data and it is important to note that actual BP_{ND} values could change if a partial volume effect correction would have been performed. However, many uncertainties may affect accuracy and precision of (MRI-based) partial volume effect corrections, such as co-registration and segmentation errors, together with the actual MRI scanner and sequence being used (Kloet *et al*., 2006). In addition, at present no partial volume effect correction method has been validated for (*R*)-[^{11}C]verapamil studies. It is expected that atrophy would result in lower BP_{ND} values of (*R*)-[^{11}C]verapamil in patients with Alzheimer's disease due to increased partial volume effects in this group. Therefore, the actual increase of (*R*)-[^{11}C]verapamil accumulation in Alzheimer's disease may have been underestimated.

The strength of this study is that it is the first to directly compare patients with Alzheimer's disease with healthy age-matched controls with the P-glycoprotein substrate tracer (*R*)-[^{11}C]verapamil. Dynamic PET studies were performed with arterial blood sampling and full kinetic modelling, providing quantitative data on P-glycoprotein function in patients with Alzheimer's disease with confirmed amyloid pathology and healthy controls. Results strongly suggest decreased P-glycoprotein function in Alzheimer's disease.

Acknowledgements

We would like to thank the technology staff of the Department of Nuclear Medicine and PET Research for their help with the acquisition of PET data and the technology staff of the Department of Radiology for acquisition of MRI data.

Funding

European Community's Seventh Framework Programme (FP7/2007-2013) (grant number 201380); Alzheimer's Association (grant number NIRG-07-59545) and Amsterdam Brain Imaging Project (ABIP, grant number 2006-06).

References

Aizenstein HJ, Nebes RD, Saxton JA, Price JC, Mathis CA, Tsopelas ND, et al. Frequent amyloid deposition without significant cognitive impairment among the elderly. Arch Neurol 2008; 65: 1509–17.

Ambudkar SV, Dey S, Hrycyna CA, Ramachandra M, Pastan I, Gottesman MM. Biochemical, cellular, and pharmacological aspects of the multidrug transporter. Annu Rev Pharmacol Toxicol 1999; 39: 361–98.

Bain LJ, LeBlanc GA. Interaction of structurally diverse pesticides with the human MDR1 gene product P-glycoprotein. Toxicol Appl Pharmacol 1996; 141: 288–98.

Bart J, Groen HJ, Hendrikse NH, van der Graaf WT, Vaalburg W, de Vries EG. The blood–brain barrier and oncology: new insights into function and modulation. Cancer Treat Rev 2000; 26: 449–62.

Bart J, Willemsen AT, Groen HJ, van der Graaf WT, Wegman TD, Vaalburg W, et al. Quantitative assessment of P-glycoprotein function

in the rat blood–brain barrier by distribution volume of [11C]verapamil measured with PET. Neuroimage 2003; 20: 1775–82.
Bartels AL, Kortekaas R, Bart J, Willemsen AT, de Klerk OL, de Vries JJ, et al. Blood-brain barrier P-glycoprotein function decreases in specific brain regions with aging: a possible role in progressive neurodegeneration. Neurobiol Aging 2009; 30: 1818–24.
Bartels AL, van Berckel BN, Lubberink M, Luurtsema G, Lammertsma AA, Leenders KL. Blood-brain barrier P-glycoprotein function is not impaired in early Parkinson's disease. Parkinsonism Relat D 2008a; 14: 505–8.
Bartels AL, Willemsen AT, Kortekaas R, de Jong BM, de VR, de KO, et al. Decreased blood–brain barrier P-glycoprotein function in the progression of Parkinson's disease, PSP and MSA. J Neural Transm 2008b; 115: 1001–9.
Bauer M, Karch R, Neumann F, Abrahim A, Wagner CC, Kletter K, et al. Age dependency of cerebral P-gp function measured with (R)-[11C]verapamil and PET. Eur J Clin Pharmacol 2009; 65: 941–6.
Blennow K, de Leon MJ, Zetterberg H. Alzheimer's disease. Lancet 2006; 368: 387–403.
Braak H, Braak E. Neuropathological stageing of Alzheimer-related changes. Acta Neuropathol 1991; 82: 239–59.
Brix G, Zaers J, Adam LE, Bellemann ME, Ostertag H, Trojan H, et al. Performance evaluation of a whole-body PET scanner using the NEMA protocol. National Electrical Manufacturers Association. J Nucl Med 1997; 38: 1614–23.
Cirrito JR, Deane R, Fagan AM, Spinner ML, Parsadanian M, Finn MB, et al. P-glycoprotein deficiency at the blood–brain barrier increases amyloid-beta deposition in an Alzheimer disease mouse model. J Clin Invest 2005; 115: 3285–90.
Cummings JL. Alzheimer's disease. N Engl J Med 2004; 351: 56–67.
Cunningham VJ, Jones T. Spectral analysis of dynamic PET studies. J Cereb Blood Flow Metab 1993; 13: 15–23.
de Lange EC. Potential role of ABC transporters as a detoxification system at the blood-CSF barrier. Adv Drug Deliv Rev 2004; 56: 1793–809.
Deane R, Bell RD, Sagare A, Zlokovic BV. Clearance of amyloid-beta peptide across the blood–brain barrier: implication for therapies in Alzheimer's disease. CNS Neurol Disord Drug Targets 2009; 8: 16–30.
Deane R, Wu Z, Zlokovic BV. RAGE (yin) versus LRP (yang) balance regulates alzheimer amyloid beta-peptide clearance through transport across the blood–brain barrier. Stroke 2004; 35: 2628–31.
Deane R, Zlokovic BV. Role of the blood–brain barrier in the pathogenesis of Alzheimer's disease. Curr Alzheimer Res 2007; 4: 191–7.
Demeule M, Labelle M, Regina A, Berthelet F, Beliveau R. Isolation of endothelial cells from brain, lung, and kidney: expression of the multidrug resistance P-glycoprotein isoforms. Biochem Biophys Res Commun 2001; 281: 827–34.
Didziapetris R, Japertas P, Avdeef A, Petrauskas A. Classification analysis of P-glycoprotein substrate specificity. J Drug Target 2003; 11: 391–406.
Donahue JE, Flaherty SL, Johanson CE, Duncan JA III, Silverberg GD, Miller MC, et al. RAGE, LRP-1, and amyloid-beta protein in Alzheimer's disease. Acta Neuropathol 2006; 112: 405–15.
Engler H, Forsberg A, Almkvist O, Blomquist G, Larsson E, Savitcheva I, et al. Two-year follow-up of amyloid deposition in patients with Alzheimer's disease. Brain 2006; 129: 2856–66.
Fazekas F, Chawluk JB, Alavi A, Hurtig HI, Zimmerman RA. MR signal abnormalities at 1.5 T in Alzheimer's dementia and normal aging. AJR Am J Roentgenol 1987; 149: 351–6.
Folstein MF, Folstein SE, McHugh PR. "Mini-mental State". A practical method for grading the cognitive state of patients for the clinician. J Psychiatr Res 1975; 12: 189–98.
Fromm MF. Importance of P-glycoprotein at blood-tissue barriers. Trends Pharmacol Sci 2004; 25: 423–9.
Gunn RN, Sargent PA, Bench CJ, Rabiner EA, Osman S, Pike VW, et al. Tracer kinetic modeling of the 5-HT1A receptor ligand [carbonyl-11C]WAY-100635 for PET. Neuroimage 1998; 8: 426–40.
Hardy J, Selkoe DJ. The amyloid hypothesis of Alzheimer's disease: progress and problems on the road to therapeutics. Science 2002; 297: 353–6.
Hartz AM, Miller DS, Bauer B. Restoring blood–brain barrier P-glycoprotein reduces brain amyloid-beta in a mouse model of Alzheimer's disease. Mol Pharmacol 2010; 77: 715–23.
Hendrikse NH, Bart J, de Vries EG, Groen HJ, van der Graaf WT, Vaalburg W. P-glycoprotein at the blood–brain barrier and analysis of drug transport with positron-emission tomography. J Clin Pharmacol 2001; (Suppl): 48S–54S.
Hendrikse NH, de Vries EG, Eriks-Fluks L, van der Graaf WT, Hospers GA, Willemsen AT, et al. A new in vivo method to study P-glycoprotein transport in tumors and the blood–brain barrier. Cancer Res 1999; 59: 2411–6.
Innis RB, Cunningham VJ, Delforge J, Fujita M, Gjedde A, Gunn RN, et al. Consensus nomenclature for in vivo imaging of reversibly binding radioligands. J Cereb Blood Flow Metab 2007; 27: 1533–9.
Johnson KA, Gregas M, Becker JA, Kinnecom C, Salat DH, Moran EK, et al. Imaging of amyloid burden and distribution in cerebral amyloid angiopathy. Ann Neurol 2007; 62: 229–34.
Kloet RW, Berckel BNM, Pouwels PJW, Schuitemaker A, Barkhof F, Kropholler MA, et al. Effects of MR scanner type, scanning sequence and segmentation algorithm on MR-based partial volume corrections of [^{11}C](*R*)-PK11195 studies. Neuroimage 2006; 32 (Suppl 2): T83.
Klunk WE, Engler H, Nordberg A, Wang Y, Blomqvist G, Holt DP, et al. Imaging brain amyloid in Alzheimer's disease with Pittsburgh Compound-B. Ann Neurol 2004; 55: 306–19.
Kropholler MA, Boellaard R, Schuitemaker A, van Berckel BN, Luurtsema G, Windhorst AD, et al. Development of a tracer kinetic plasma input model for (R)-[11C]PK11195 brain studies. J Cereb Blood Flow Metab 2005; 25: 842–51.
Kuhnke D, Jedlitschky G, Grube M, Krohn M, Jucker M, Mosyagin I, et al. MDR1-P-Glycoprotein (ABCB1) Mediates Transport of Alzheimer's amyloid-beta peptides–implications for the mechanisms of Abeta clearance at the blood–brain barrier. Brain Pathol 2007; 17: 347–53.
Lam FC, Liu R, Lu P, Shapiro AB, Renoir JM, Sharom FJ, et al. beta-Amyloid efflux mediated by p-glycoprotein. J Neurochem 2001; 76: 1121–8.
Lammertsma AA, Hume SP. Simplified reference tissue model for PET receptor studies. Neuroimage 1996; 4: 153–8.
Lee G, Bendayan R. Functional expression and localization of P-glycoprotein in the central nervous system: relevance to the pathogenesis and treatment of neurological disorders. Pharm Res 2004; 21: 1313–30.
Lee JH, Kim SH, Kim GH, Seo SW, Park HK, Oh SJ, et al. Identification of pure subcortical vascular dementia using 11C-Pittsburgh compound B. Neurology 2011; 77: 18–25.
Lee YJ, Maeda J, Kusuhara H, Okauchi T, Inaji M, Nagai Y, et al. In vivo evaluation of P-glycoprotein function at the blood–brain barrier in nonhuman primates using [11C]verapamil. J Pharmacol Exp Ther 2006; 316: 647–53.
Loscher W, Potschka H. Blood-brain barrier active efflux transporters: ATP-binding cassette gene family. NeuroRx 2005; 2: 86–98.
Lubberink M, Luurtsema G, van Berckel BN, Boellaard R, Toornvliet R, Windhorst AD, et al. Evaluation of tracer kinetic models for quantification of P-glycoprotein function using (R)-[11C]verapamil and PET. J Cereb Blood Flow Metab 2007; 27: 424–33.
Luurtsema G, Molthoff CF, Schuit RC, Windhorst AD, Lammertsma AA, Franssen EJ. Evaluation of (R)-[11C]verapamil as PET tracer of P-glycoprotein function in the blood–brain barrier: kinetics and metabolism in the rat. Nucl Med Biol 2005; 32: 87–93.
Luurtsema G, Molthoff CF, Windhorst AD, Smit JW, Keizer H, Boellaard R, et al. R)- and (S)-[11C]verapamil as PET-tracers for measuring P-glycoprotein function: in vitro and in vivo evaluation. Nucl Med Biol 2003; 30: 747–51.
Luurtsema G, Windhorst AD, Mooijer MP, Herscheid JD, Lammertsma AA, Franssen EJ. Fully automated high yield synthesis

of (R)- and (S)-[C-11]verapamil for measuring P-glycoprotein function with positron emission tomography. J Labelled Compds Radiopharm 2002; 45: 1199–207.

Mawuenyega KG, Sigurdson W, Ovod V, Munsell L, Kasten T, Morris JC, et al. Decreased clearance of CNS beta-amyloid in Alzheimer's disease. Science 2010; 330: 1774.

McKhann G, Drachman D, Folstein M, Katzman R, Price D, Stadlan EM. Clinical diagnosis of Alzheimer's disease: report of the NINCDS-ADRDA Work Group under the auspices of Department of Health and Human Services Task Force on Alzheimer's Disease. Neurology 1984; 34: 939–44.

Muzi M, Mankoff DA, Link JM, Shoner S, Collier AC, Sasongko L, et al. Imaging of cyclosporine inhibition of P-glycoprotein activity using 11C-verapamil in the brain: studies of healthy humans. J Nucl Med 2009; 50: 1267–75.

Ossenkoppele R, Tolboom N, Foster-Dingley JC, Boellaard R, Yaqub M, Windhorst AD, et al. Time Course of specific [^{11}C]PIB and [^{18}F]FDDNP binding: paired studies in patients with Alzheimer's disease, mild cognitive impairment and healthy controls. Neuroimage 2010; 52 (Suppl 1): \$52.

Pike KE, Savage G, Villemagne VL, Ng S, Moss SA, Maruff P, et al. Beta-amyloid imaging and memory in non-demented individuals: evidence for preclinical Alzheimer's disease. Brain 2007; 130: 2837–44.

Sasongko L, Link JM, Muzi M, Mankoff DA, Yang X, Collier AC, et al. Imaging P-glycoprotein transport activity at the human blood–brain barrier with positron emission tomography. Clin Pharmacol Ther 2005; 77: 503–14.

Schinkel AH. P-Glycoprotein, a gatekeeper in the blood–brain barrier. Adv Drug Deliv Rev 1999; 36: 179–94.

Smith EE, Greenberg SM. Beta-amyloid, blood vessels, and brain function. Stroke 2009; 40: 2601–6.

Svarer C, Madsen K, Hasselbalch SG, Pinborg LH, Haugbol S, Frokjaer VG, et al. MR-based automatic delineation of volumes of interest in human brain PET images using probability maps. Neuroimage 2005; 24: 969–79.

Tolboom N, van der Flier WM, Boverhoff J, Yaqub M, Wattjes MP, Raijmakers PG, et al. Molecular imaging in the diagnosis of Alzheimer's disease: visual assessment of [11C]PIB and [18F]FDDNP PET images. J Neurol Neurosurg Psychiatry 2010; 81: 882–4.

Tolboom N, Yaqub M, Boellaard R, Luurtsema G, Windhorst AD, Scheltens P, et al. Test-retest variability of quantitative [11C]PIB studies in Alzheimer's disease. Eur J Nucl Med Mol Imaging 2009a; 36: 1629–38.

Tolboom N, Yaqub M, van der Flier WM, Boellaard R, Luurtsema G, Windhorst AD, et al. Detection of Alzheimer pathology in vivo using both 11C-PIB and 18F-FDDNP PET. J Nucl Med 2009b; 50: 191–7.

Toornvliet R, van Berckel BN, Luurtsema G, Lubberink M, Geldof AA, Bosch TM, et al. Effect of age on functional P-glycoprotein in the blood–brain barrier measured by use of (R)-[(11)C]verapamil and positron emission tomography. Clin Pharmacol Ther 2006; 79: 540–8.

Tournier N, Valette H, Peyronneau MA, Saba W, Goutal S, Kuhnast B, et al. Transport of selected PET radiotracers by human P-glycoprotein (ABCB1) and breast cancer resistance protein (ABCG2): an in vitro screening. J Nucl Med 2011; 52: 415–23.

Uhr M, Grauer MT. abcb1ab P-glycoprotein is involved in the uptake of citalopram and trimipramine into the brain of mice. J Psychiatr Res 2003; 37: 179–85.

Uhr M, Steckler T, Yassouridis A, Holsboer F. Penetration of amitriptyline, but not of fluoxetine, into brain is enhanced in mice with blood–brain barrier deficiency due to mdr1a P-glycoprotein gene disruption. Neuropsychopharmacology 2000; 22: 380–7.

Vogelgesang S, Cascorbi I, Schroeder E, Pahnke J, Kroemer HK, Siegmund W, et al. Deposition of Alzheimer's beta-amyloid is inversely correlated with P-glycoprotein expression in the brains of elderly non-demented humans. Pharmacogenetics 2002; 12: 535–41.

Vogelgesang S, Warzok RW, Cascorbi I, Kunert-Keil C, Schroeder E, Kroemer HK, et al. The role of P-glycoprotein in cerebral amyloid angiopathy; implications for the early pathogenesis of Alzheimer's disease. Curr Alzheimer Res 2004; 1: 121–5.

Wagner CC, Bauer M, Karch R, Feurstein T, Kopp S, Chiba P, et al. A pilot study to assess the efficacy of tariquidar to inhibit P-glycoprotein at the human blood–brain barrier with (R)-11C-verapamil and PET. J Nucl Med 2009; 50: 1954–61.

Weller RO, Subash M, Preston SD, Mazanti I, Carare RO. Perivascular drainage of amyloid-beta peptides from the brain and its failure in cerebral amyloid angiopathy and Alzheimer's disease. Brain Pathol 2008; 18: 253–66.

Yaqub M, Tolboom N, Boellaard R, van Berckel BN, van Tilburg EW, Luurtsema G, et al. Simplified parametric methods for [11C]PIB studies. Neuroimage 2008; 42: 76–86.

Zlokovic BV, Yamada S, Holtzman D, Ghiso J, Frangione B. Clearance of amyloid beta-peptide from brain: transport or metabolism? Nat Med 2000; 6: 718.